Sustainable Energy & Fuels

ROYAL SOCIETY OF CHEMISTRY

PAPER

View Article Online
View Journal | View Issue



Cite this: *Sustainable Energy Fuels*, 2024, **8**, 5568

# Advanced atmospheric pressure CVD of a-Si:H using pure and cyclooctane-diluted trisilane as precursors†

Benedikt Fischer, *[ab] Maurice Nuys,[ac] Oleksandr Astakhov,[a] Stefan Haas,[ad] Michael Schaaf,[e] Astrid Besmehn,[f] Peter Jakes,[g] Rüdiger-A. Eichel[gh] and Uwe Rau[ab]

Liquid silanes can be used for low-cost, fast deposition of hydrogenated amorphous silicon (a-Si:H) as an alternative to state-of-the-art deposition processes such as plasma enhanced chemical vapor deposition or electron beam evaporation. However, liquid silane deposition techniques are still in their infancy. In this paper, we present a new version of the atmospheric pressure chemical vapor deposition technique designed to improve the reproducibility of a-Si:H deposition. With this new tool, we explore ways to improve the quality of the material. The films can be prepared using pure trisilane as a precursor; frequently, however, trisilane is diluted with cyclooctane for better handling and process control. Currently, the influence of this dilution on the film quality is not well understood. In our work, we investigate and compare both precursor strategies. This paper presents a comprehensive analysis of the effects of cyclooctane dilution, deposition temperature, process duration, and precursor amount on the structure stoichiometry and electronic properties of the resulting films. The analysis was performed using a range of techniques, including Fourier transform infrared spectroscopy, electronic spin resonance spectroscopy, Raman spectroscopy, ellipsometry, secondary ion mass spectrometry, and conductivity measurements. For films deposited with pure silane, we found a low oxygen (O) and carbon (C) impurity incorporation and an adjustable H content up to 10%, resulting in a photosensitivity of up to $10^4$. Dependent on the dilution and deposition temperature, the films deposited with cyclooctane dilution showed various amounts of C incorporation, culminating in an a-Si:H/a-SiC:H structure for high temperatures and dilutions. High purity a-Si:H films as a-Si:C:H films are promising for application in solar cells and transistors either as an amorphous functional layer or as a precursor for recrystallization processes, *e.g.*, in TOPCon solar cell technology.

Received 20th September 2024
Accepted 18th October 2024

DOI: 10.1039/d4se01308e

rsc.li/sustainable-energy



## Introduction

Hydrogenated amorphous silicon thin films used in transistors, batteries and solar cells are usually prepared with relatively expensive processes such as plasma enhanced chemical vapor deposition (PECVD), hot wire chemical vapor deposition (HWCVD) or electron beam evaporation.[1–4] Therefore, investigations on low-cost deposition processes were made in the past.[2,5–10] One concept is to use liquid precursors such as trisilane (TS) or cyclopentasilane (CPS) and deposit it *via* low-cost deposition processes such as spin-coating or atmospheric pressure chemical vapor deposition (APCVD).[5,7–13] In contrast to gaseous precursors, liquid precursors have the advantage of a wide applicability in solution and also in vapor-processes. They do not need high pressure gas canisters or carrier tubes for storage because of their liquid state.[8,14] In addition, liquid precursors can be used for local deposition processes or other specialized processes such as Si deposition in nanopores.[12] Original experiments on APCVD deposition were successful in proof of principle; however, they had reproducibility and process control issues.[10] In this work, we

[a]*IEK-5 Photovoltaik, Forschungszentrum Jülich GmbH, Wilhelm-Johnen Straße, 52425 Jülich, Germany. E-mail: b.fischer@fz-juelich.de*
[b]*Jülich Aachen Research Alliance (JARA-Energy), Faculty of Electrical Engineering and Information Technology, RWTH Aachen University, Schinkelstr. 2, 52062 Aachen, Germany*
[c]*Department of Energy Building Services Environmental Engineering, University of Applied Sciences Muenster, Stegerwaldstraße 39, 48565 Steinfurt, Germany*
[d]*Department of Aerospace Engineering, FH Aachen University of Applied Sciences, 52066 Aachen, Germany*
[e]*ZEA-1 Engineering und Technologie, Forschungszentrum Jülich GmbH, Wilhelm-Johnen Straße, 52425 Jülich, Germany*
[f]*IEK-14 Elektrochemische Verfahrenstechnik, Forschungszentrum Jülich GmbH, Wilhelm-Johnen Straße, 52425 Jülich, Germany*
[g]*IEK-9 Grundlagen der Elektrochemie, Forschungszentrum Jülich GmbH, Wilhelm-Johnen Straße, 52425 Jülich, Germany*
[h]*Institute of Physical Chemistry, RWTH Aachen University, 52074 Aachen, Germany*

† Electronic supplementary information (ESI) available. See DOI: https://doi.org/10.1039/d4se01308e

present a new version of the APCVD apparatus designed to improve the reproducibility of the deposition and capability of using untreated trisilane and cyclooctane-diluted trisilane as precursors. With this new tool, we explore a large process parameter space, seeking to improve the quality of the deposited thin film Si films.

A number of studies have been carried out on the deposition of a-Si:H using liquid precursors such as trisilane often diluted using the solvent cyclooctane for better handling.[5,6,11] Cyclooctane was used as a suitable widely available solvent with a stable carbon ring, which is important to avoid carbon contamination of amorphous Si films. However, to the best of our knowledge, there is little to no data on the actual influence of cyclooctane on the carbon content or film structure. Therefore, in our study, we investigate the effect of cyclooctane dilution on the a-Si:H film properties by changing the dilution ratio from 0 to 99% in the deposition process. The entire deposition parameter space comprises four dimensions: cyclooctane dilution, deposition temperature, deposition time, and precursor amount. To elucidate the influence of multiple process parameters on film properties, we employ a set of characterization techniques: spectroscopic ellipsometry for thickness; electron spin resonance (ESR) spectroscopy for paramagnetic states and defects; secondary ion mass spectrometry (SIMS) for atomic composition; a custom-built setup for electrical conductivity; Raman spectroscopy for structural analysis; and Fourier transform infrared (FTIR) spectroscopy for the H content $c_H$, the Si–H bonding configuration and the incorporation of carbon.

The study is organized and presented as follows. First, the effects of deposition temperature, deposition time, and precursor amount are examined in films prepared with pure trisilane as a precursor. A comparison to a reference intrinsic a-Si:H film deposited by PECVD allows us to explore the potential a-Si:H material quality achievable through the new deposition method. In the second part of the paper, we analyze the effects of cyclooctane dilution, with particular emphasis on the potential incorporation of carbon and the resulting impact on the quality of the deposited material. For undiluted trisilane there are regions of parameters delivering intrinsic films with high photosensitivity potentially applicable as passivation layers in solar cells and other regions yielding films with low H content suitable for blistering-free crystallization processes. For the diluted precursor, we can see incorporation of carbon, which strongly depends on substrate temperature. At temperatures below 495 °C, only minor contamination is detected, negligible for the electronic film properties, whereas at higher temperatures, the carbon content increases significantly reaching up to $10^{22}$ atoms per $cm^3$ at 580 °C which puts the resulting films into the category of silicon carbide alloys. In this case, the technique can find its applications for atmospheric pressure preparation of SiC.

## Experimental details

### Preparation technique

In an APCVD process, thin films of a-Si:H are deposited onto a heated substrate under atmospheric pressure by means of pyrolysis out of the gas phase. The technical drawing and a schematic of our novel dedicated APCVD system are shown in Fig. 1. For impurity protection and to prevent a reaction between trisilane and $O_2$, the system is built up in a glove box from MBraun filled with nitrogen ($O_2$, $H_2O$ <1 ppm). The glove box located in an air-conditioned room makes the process independent of ambient temperature and humidity. Only the ambient pressure has a little influence on the deposition pressure, since the glove box pressure approximately corresponds to the ambient pressure plus 3 mbar. Since the changes in the ambient pressure due to different weather conditions are small compared to the absolute pressure, their influence is not considered here. As a heat source, we used an Isotemp hot plate from Fisherbrand. The hot plate heats a (6 × 6) $cm^2$ stainless steel block and a (10 × 10) $cm^2$ quartz glass plate with 1 mm thickness on top of the steel block. The glass prevents contamination of the (1.5 × 1.5) $cm^2$ sample substrates (c-Si wafer or glass) by diffusion of atoms from the steel block to the substrate. The steel block is used to conduct the heat on to an area of (6 × 6) $cm^2$ on the glass plate because the precursor only reacts at the hot surface areas with $T$ > 400 °C. Thermocouples are used to monitor the temperature of the steel block and precursor inlet block. The temperature of the steel block is used as "deposition temperature" $T$ within this work. On top of the hot plate, a height adjustable head lowered to the hotplate during the process creates a closed deposition chamber. No special sealing was included, since no vacuum is needed. The precursor is pumped into a tube on top of the chamber-head using a dosage pump with at least 5 µl dosage strokes and then flushed out into the chamber by opening a magnetic valve for 0.1–1 s. In the chamber, the precursor sprays onto a baffle plate and evaporates, as indicated in Fig. 1b. Within the gas phase, the precursor is distributed in the chamber, decomposes at the hot substrate surface, and deposits as a thin a-Si:H film on the substrate. To ensure that the precursor is in the liquid phase during pumping/flushing, the inlet block including the precursor reservoir is cooled using a Peltier element to temperatures below 30 °C, well below the boiling point of trisilane of 53 °C (at 1013 hPa).[15] To produce our precursor solutions, we used trisilane from Voltaix LLC (Silcore®, 99.99% purity) and cyclooctane from Sigma-Aldrich (99.0% purity). For the samples deposited with the 2% trisilane (98% cyclooctane) solution, the insertion *via* the dosage pump was very reproducible. For the pure trisilane depositions and dilution series, the dosage of the precursor *via* the dosage pump was not possible due to the small precursor volume. Therefore, the precursor was dosed per Eppendorf pipette and then by opening the dosage pump, the precursor was flushed into the chamber with nitrogen for 1 second. The magnetic valve, shown in Fig. 1b, was closed during flushing. This procedure leads to higher fluctuation of the actual amount of the precursor within the deposition chamber and, therefore, to a higher fluctuation of the film thicknesses. After waiting for a certain time herein called "deposition time" to grow the film, the deposition process is finished by lifting the deposition chamber and removing the samples from the hot plate.

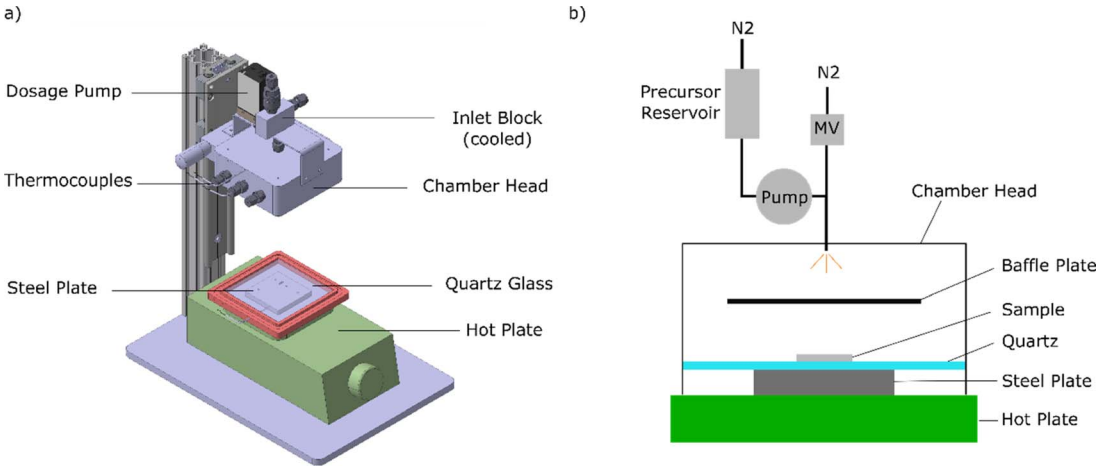


Fig. 1 (a) Technical drawing and (b) schematic of the APCVD system.

Table 1 Deposition parameters of the here analyzed sample series. The parameter which was varied is shown in bold. The proportion of trisilane in the precursor (TS content) is given in percent by volume. In addition, the deposition temperature and time are given, as well as the total precursor amount including trisilane and solvent (amount)

| Series | TS content [%] | Temperature [°C] | Time [min] | Amount [μl] |
|---|---|---|---|---|
| Temp1 | 100 | **410–580** | 10 | 10 |
| Time1 | 100 | 440, 555 | **10, 20, 50** | 20 |
| Amount1 | 100 | 440, 555 | 10 | **10, 20, 50** |
| ESR | 100 | 440, 495, 555 | 10, 20 | 10, 20 |
| SIMS | 100 | 440, 495, 555 | 10, 20 | 10, 20 |
| Dilution | **1–100** | 440, 495, 555 | 10 | 10–1000 |
| Temp2 | 2 | **410–580** | 10 | 400 |
| Time2 | 2 | 470 | **1-50** | 400 |
| Amount2 | 2 | 470 | 10 | **200–1000** |

Using this setup, nine sample series have been prepared. As summarized in Table 1 the sets of samples are separated into two major groups for materials prepared with pure trisilane and diluted trisilane. In both cases, we aimed to test a wide range of deposition parameters. The primary investigated parameter in each group of samples is shown in bold. For pure trisilane the series "Temp1", "Time1", and "Amount1" a variation of one deposition parameter (deposition temperature, time or precursor amount respectively) is investigated. The samples were characterized mainly by FTIR spectroscopy, ellipsometry and conductivity measurements. For the ESR and SIMS measurements, two extra series called "ESR" and "SIMS" were prepared. In the sixth series "Dilution" the trisilane content diluted in cyclooctane used as the precursor was changed from 1 to 100% at three different temperatures. The last three series, "Temp2", "Time2", and "Amount2" again focus on the variation of deposition temperature, time or precursor amount respectively, but using 2% trisilane diluted in cyclooctane as the precursor.

## Characterization

For the analysis, each film was co-deposited simultaneously on a (15 × 15) $mm^2$ polished p-type high resistivity c-Si (100) float-zone wafer (525 μm, 20 Ω cm) with native oxide and on a (15 × 15) $mm^2$ Corning glass type Eagle 2000.

The film thickness is measured by spectroscopic ellipsometry using a T-Solar/M2000 from J.A. Woollam.

The Si bonding structure is analyzed using FTIR using a Nicolet 5700 system from Thermo Electron Corporation.

To calculate the bond-density, we used the absorption strengths by Beyer and Ghazala[16] for the Si–H and by Kaneko *et al.*[17] for the Si–C stretching vibrations. We calculated the microstructure parameter $R$, which is often used to describe the microstructure of a-Si:H films according to the method published previously in ref. 18. $R$ is the ratio of the integrated peak areas of Si–H vibrations contributing to peaks near 2100 $cm^{-1}$ and 2000 $cm^{-1}$, corresponding to H bonded in void-rich and dense materials, respectively.[16,19–21] Adding carbon to a-Si:H films can increase the peak near 2100 $cm^{-1}$ and therefore the $R$, since vibrations of Si–H bonds with a carbon back-bond on the silicon atom are also located near the 2100 $cm^{-1}$ peak.[22] We used this fact together with the Si–C vibration peak located at 780 $cm^{-1}$ and SIMS measurements to investigate the carbon content in the a-Si:H films deposited with trisilane diluted in cyclooctane.

To investigate the chemical composition, we performed SIMS measurements using the time-to-flight setup ToF-SIMS5.ncs from IONTOF GmbH with a cesium sputtering beam and a sputtering energy of 1 keV on an area of (300 × 300) $μm^2$. We compare the SIMS measurement of the APCVD films with an intrinsic a-Si:H reference film deposited by PECVD with the recipe for the passivating i1-layer used in SHJ solar cells.[23] The dark and photoconductivity $\sigma_d$ and $\sigma_{ph}$, respectively, of our film is measured using a home-made system. The light source was a mercury lamp calibrated to an intensity of one sun.

Electron spin resonance (ESR) measurements (a.k.a. electron paramagnetic resonance – EPR) are made in conventional continuous wave (CW) mode using a commercial X-band ($\nu$ = 9.8 GHz) Bruker ELEXSYS E-500 system in an ER 4108 TMHS resonator at room temperature. Two identical pieces of the thin film on a Corning glass substrate cut in (5 × 5) $mm^2$ pieces were fixed face-to-face with scotch tape on the tip of a 4 mm diameter

 

quartz sample tube and positioned in the center of an opaque resonator cavity. To ensure that the substrate or holder does not contribute to the detected signal, a reference measurement was made on substrates without sample films, which showed a negligible baseline compared to the signal detected from the films under test. A calibrated sample of sputtered amorphous silicon with a spin number of $2 \times 10^{15}$ and $g$-value of 2.00565 was used as a reference secondary standard[24] for calibration of the magnetic field and signal intensity for further $g$-value and spin density evaluation in measured samples. The spectra were measured at a microwave power of 0.1 mW, a sweep width of 100 G, a magnetic field modulation at a frequency of 100 kHz and an amplitude of 3 G. It was confirmed that no saturation or over modulation effects occur under these conditions.

## Results

### Material deposited using pure trisilane as the precursor

The APCVD films deposited using pure trisilane with a variation of substrate temperature, deposition time and precursor amount (series Temp1, Time1 and Amount1 outlined in Table 1) have been characterized with several spectroscopic techniques such as FTIR, Raman and ESR spectroscopy. For all three methods, we observed spectra/signatures typical for amorphous silicon prepared by traditional techniques. *e.g.*, the FTIR spectra contain peaks at 640 $cm^{-1}$ and 2000 $cm^{-1}$ typical for a-Si:H and overall, the spectra are typical for a-Si:H prepared with PECVD, HWCVD, sputtering or APCVD techniques.[7,16,25,26] Therefore, we identify the material as a-Si:H and use this notation throughout the manuscript.

Dark and photoconductivity $\sigma_d$ and $\sigma_{ph}$, thickness $d$, H content and microstructure parameter $R$ of the pure silane samples of series Temp1, Time1 and Amount1 are summarized in Fig. 2.

Fig. 2a shows the results for samples of series Temp1. The film thickness of the a-Si:H films strongly increases with increasing hot plate temperatures between 410 °C and 495 °C due to a higher growth rate, in agreement with the literature.[27] At 495 °C, a plateau is reached, likely indicating the complete deposition of the injected precursor. The thickness decreases slightly for temperatures of 555 °C and 580 °C, which can be attributed to two effects. (i) The major effect is a larger area that is unintentionally heated up to temperatures allowing the deposition of a-Si:H (*e.g.*, at the walls of the deposition chamber). A larger deposition area at the same precursor amount leads to thinner films on the substrate if the growth process is limited by the precursor amount and not by deposition time. (ii) A minor effect is that $c_H$ decreases from 4% at $T =$ 440 °C to below 1% at $T >$ 525 °C due to hydrogen effusion, which can also lead to a small shrinking effect of the a-Si:H films with higher temperature.[28,29]

The conductivity measurement results in Fig. 2a show a split of $\sigma_{ph}$ and $\sigma_d$ for temperatures $T \leq$ 495 °C. In this range, the logarithm of $\sigma_{ph}$ qualitatively follows the curve of $c_H$. For temperatures above 495 °C, $\sigma_d$ increases to values nearly equal to those of $\sigma_{ph}$. At these higher temperatures, $c_H$ drops significantly to below 1%. The conductivity continues to increase with increasing deposition temperature, surpassing $10^6$ S $cm^{-1}$. This increase may be attributed to a higher density of defects, which could enhance hopping conductivity and might lead to the formation of a conductive defect band. The ratio of $\sigma_{ph}$ to $\sigma_d$, known as photosensitivity, is often used to assess the quality of intrinsic a-Si for optoelectronic applications.[30–32] The highest photosensitivity, $2.5 \times 10^2$, was observed at 470 °C in the Temp1 series shown in Fig. 2a. The microstructure parameter is below 0.1 for all films, except for the film deposited at 410 °C. The low $R$ for films deposited at $T >$ 410 °C can result from two different material properties. (i) It can result from the dense material with H bonded mainly within the Si-network.[25,33] (ii) It can result

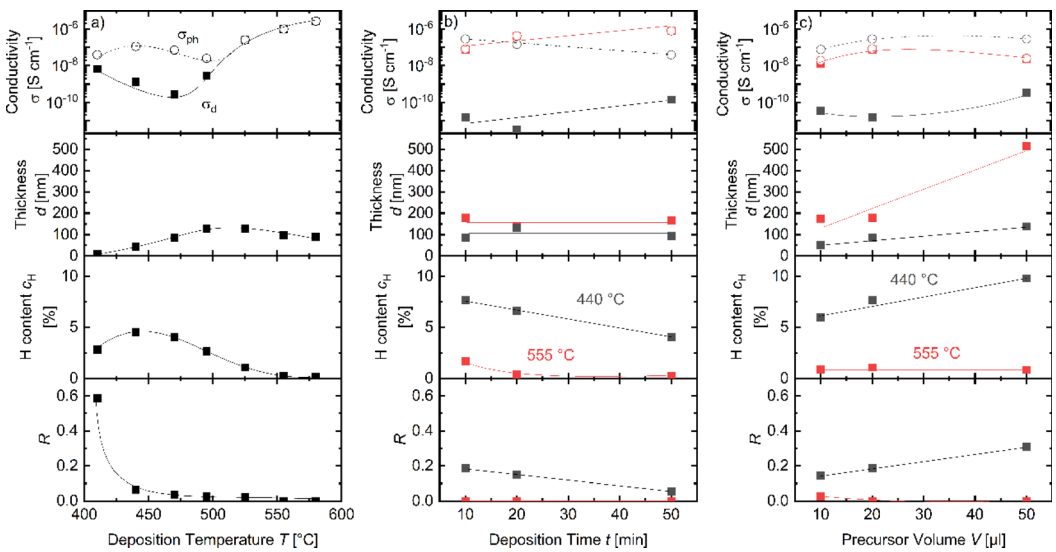


Fig. 2 Dark and photoconductivity $\sigma_d$ and $\sigma_{ph}$, thickness $d$, hydrogen content $c_H$ and microstructure parameter $R$ of a-Si:H films deposited with pure trisilane as a precursor as a function of (a) deposition temperature $T$, (b) deposition time $t$, and (c) precursor volume $V$. $t$ and $V$ were varied at temperatures $T =$ 440 °C (gray) and 555 °C (red). The lines are guides to the eye.

from the void-rich material where H bonded in voids effused during the deposition process, since the deposition temperature is above the effusion peak temperature at approximately 385 °C of H in voids, but below that of H within the Si network.[34] Because of the absence of the H in the voids which would contribute to the 2100 $cm^{-1}$ peak, this could result in a low $R$ despite the presence of voids in the material. The increased $R$ for the film deposited at 410 °C might be a relic of the low film thickness of $d = 9$ nm. For low a-Si:H film thicknesses, the amount of H within the bulk a-Si:H can be in the same order of magnitude as the amount of the H bonded at the interface between a-Si:H and c-Si. The interface H can contribute significantly to the 2100 $cm^{-1}$ peak, leading to a higher $R$.[18]

The hydrogen effusion during deposition is examined in more detail in the Time1 series, where 20 µl of trisilane was injected at 440 °C and 555 °C for durations of 10, 20, and 50 minutes. The results of this series are displayed in Fig. 2b. For $T_d = 440$ °C, $c_H$ and $R$ decrease with longer deposition times. Specifically, $c_H$ drops from 8% to 4%, and $R$ decreases from 0.2 to 0.05. This suggests that hydrogen bonded in a more porous or void-rich structure (associated with the 2100 $cm^{-1}$ peak) indeed effuses out of the film over time. As the deposition time increases, $\sigma_d$ increases while $\sigma_{ph}$ decreases. This trend is consistent with a higher density of defects and a lower hydrogen content, both of which contribute to a lower $\sigma_{ph}$ and, consequently, reduced photosensitivity.[35,36] For $T_d = 555$ °C, $c_H$ falls below 2%, and $R$ is approximately 0, as the 2100 $cm^{-1}$ peak is near or below the detection limit. Both $\sigma_{ph}$ and $\sigma_d$ are almost equal, and both increase with longer deposition times. These observations suggest that the effusion of hydrogen and the resulting changes in the film's microstructure and defect density significantly influence the conductivity and photosensitivity of the material.

The effect of the injected precursor amount has been investigated by preparing the sample series Amount1, whose measurement results are shown in Fig. 2c. For two deposition temperatures, $T = 440$ °C and $T = 555$ °C, we used precursor amounts of 10, 20 and 50 µl trisilane. Increasing the amount of precursor results in increased film thickness, which is accompanied by noticeable scatter in the data, presumably due to uncertainties in precursor injection.

For $T = 440$ °C, $R$ and $c_H$ increase with increasing precursor volume. The conductivity measurements show for all precursor amounts a high photosensitivity up to $10^4$. The photoconductivity of the films deposited at $T = 440$ °C shows a slight correlation with the H contents of the films, which could already be seen in Fig. 2a and b for temperatures below 495 °C. For the deposition at $T = 555$ °C, the growth rate is higher than that for the deposition with $T = 440$ °C. However, the high temperature probably leads to a high effusion rate, leading to a low $c_H$ and low $R$ for all film thicknesses. Accordingly, the photosensitivity of all films deposited at $T = 555$ °C is ~1.

The surface profile of the a-Si:H thin films is dependent on the growth-temperature and thickness of the films. Regarding the films from the series in Fig. 2a for $T = 410$ °C and $T = 440$ °C, a flat surface without holes is obtained, as shown representatively for $T = 440$ °C in Fig. 3a. No signs of blistering have been

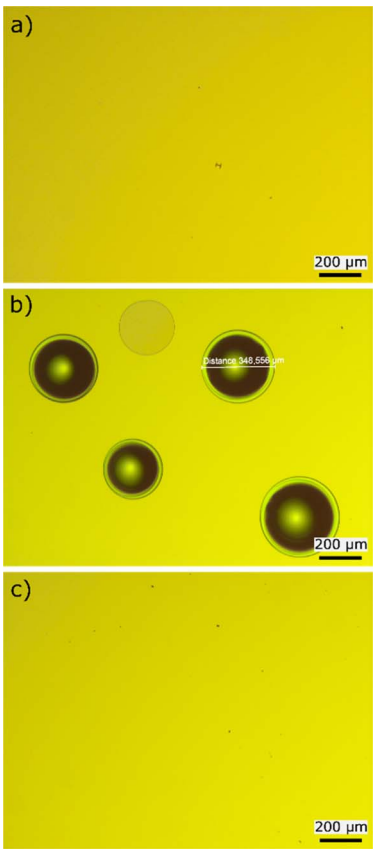


Fig. 3 Pictures made with a light microscope at five times magnification of a-Si:H films deposited at a plate temperature of (a) 440 °C, (b) 495 °C and (c) 555 °C.

observed, maybe due to a combination of small film thickness and a low H-diffusion rate. At $T = 495$ °C, shown in Fig. 3b, we observed circular holes. These were found also for the depositions at $T = 470$ and 525 °C. We attribute the formation of these holes to blistering due to $H_2$ cumulated in voids within the film or at the interface to the c-Si substrate.[37] For $T = 555$ °C and 580 °C, the surface is flat again (shown in Fig. 3c). As a matter of speculation, this might result from a loose film structure with micropores in which the hydrogen can easily effuse without accumulation and subsequent blistering. Also, it is possible that at higher temperatures hydrogen is ejected from the surface before it can incorporate into the bulk of the material.

Another possible explanation for smooth H effusion without blistering is related to the growth of crystalline structures within the material. These crystalline structures are expected to reveal themselves in Raman spectra. However, the spectra shown in Fig. 4 show a clear peak at 480 $cm^{-1}$ for all deposition temperatures, indicating that the material is amorphous and not crystalline.[26,38,39] For a deposition temperature of 525 °C, the peak is slightly shifted to higher wavenumbers which can be attributed to a more dense material or the onset of nanocrystalline growth, which is often observed in this temperature regime for longer annealing times.[40–42]

Paramagnetic electronic states in the APCVD a-Si:H films were analyzed *via* ESR spectroscopy. The deposition parameters

 

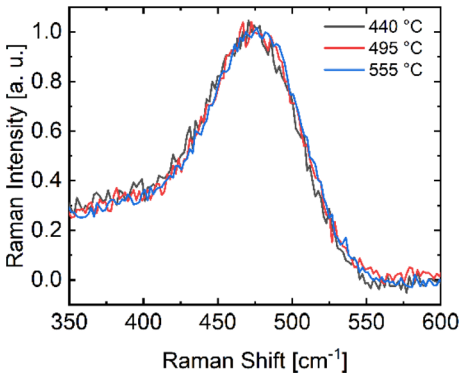


Fig. 4 Raman spectra showing the typical peak of Si–Si vibrations in amorphous silicon at 480 cm$^{-1}$ of a-Si:H films deposited at 440, 495 and 555 °C.

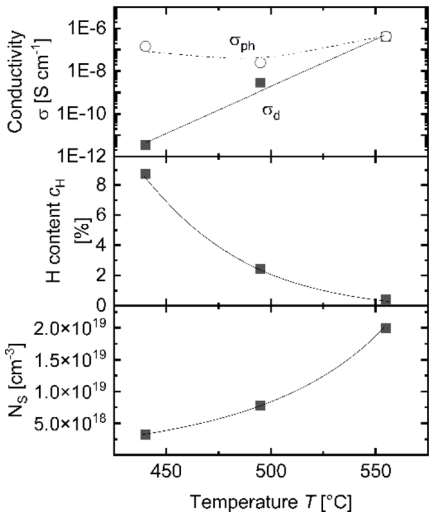


Fig. 5 Dark and photoconductivity $\sigma_d$ and $\sigma_{ph}$, hydrogen content $c_H$ and spin density $N_s$ of a-Si:H films deposited with pure trisilane as the precursor as a function of deposition temperature $T$. The lines are guides to the eye.

of these 3 samples are shown in Table 1 in the "ESR" row. It is widely accepted that the ESR signal detected in the undoped amorphous silicon originates from Si dangling bonds causing defect states within the band gap.[35,43] The ESR spectra given in ESI Fig. S1a† show a pronounced featureless, slightly asymmetric single line at a g-value of approx. 2.0055 – typical for dangling bonds in amorphous silicon.[35,43] Both the intensity of the line and, indirectly, the *g*-value point to a material with a high density of dangling bond defects.[35] The density of dangling bonds is crucial for the electronic quality of a-Si:H. It has been shown by Astakhov *et al.*[35] that photoconductivity is inversely dependent on the spin density in a-Si:H. At the same time, hydrogen passivation can effectively reduce the density of dangling bonds and improve the electronic quality of a-Si:H. Fig. 5 shows the conductivity, H-content and ESR spin density for the three a-Si:H samples with similar thicknesses (~130 nm) as a function of the hot plate temperature. With increasing temperature, $c_H$ measured by FTIR decreases. This is in line with the increase in the density of dangling bonds detected as an increase in the spin-density $N_S$ measured by ESR.[35,44] The high amount of dangling bonds can lead to an increase of the $\sigma_d$ and can be responsible for the reduction of $\sigma_{ph}$ in agreement with the trends observed in a-Si:H prepared by the traditional methods.[35,45]

Fig. 6 shows SIMS depth profiles of the a-Si:H films deposited at 440, 495 and 555 °C and a reference intrinsic a-Si:H film, deposited by PECVD. The samples have similar thicknesses *d* between 130 and 180 nm. In comparison to the reference high quality PECVD material, the APCVD material deposited at 440 °C shows similar purity with comparable C and O contents to the reference PECVD film. However, the H content in the APCVD sample is lower and less homogeneously distributed over the film thickness. The amount of H decreases near the surface as well as near the interface of the c-Si substrate. Such kind of H distribution was reported for PECVD a-Si:H films exposed to post deposition annealing.[46] Therefore, we attribute the inhomogeneous hydrogen distribution in the APCVD material to the out diffusion at 440 °C. The SIMS profiles in APCVD films prepared at higher temperatures confirm the decrease of the H content with the temperature increase detected by the FTIR measurements. Simultaneously, the increase in the deposition temperature leads to an increase in C and O content within the film. These impurities can contribute to the increase in the number of defect states.[47] The O and C counts increase near the surface, especially for $T = 495$ °C and $T = 555$ °C, indicating a higher impurity incorporation with lower precursor content within the deposition chamber.

## Material deposited using various trisilane-cyclooctane solutions

Cyclooctane is often used in APCVD as a solvent for easier handling and growth rate control.[5,6,11,13] To study the influence of cyclooctane on the film properties, we deposited films with trisilane concentrations in percentage by volume of 1 to 100% diluted in cyclooctane at temperatures of 440, 495 and 555 °C. Deposition parameters for the "Dilution" sample series are summarized in Table 1. The film properties were investigated in the same way as that for pure trisilane presented above. The FTIR spectra of the "Dilution" series samples were additionally analyzed for carbon related IR-vibrations. Fig. 7 shows a comparison of the FTIR spectra of (a) a film deposited with pure trisilane and (b) a film deposited with 2% trisilane diluted in cyclooctane. As shown in Fig. 7a the most dominant peaks arise from Si–H bending and stretching vibrations at 640 and 2100 cm$^{-1}$.[16] Additionally, from 900 to 1100 cm$^{-1}$ there are Si–O vibrations, either because of impurities or because of the native oxide on the surfaces of the c-Si substrates.[48–50] In the same region, Si–C–$H_2$ wagging modes can be found.[17,22] The sample in Fig. 7b shows Si–C vibrations at 720–780 cm$^{-1}$ and C–H vibrations at around 2850–2950 cm$^{-1}$, which clearly shows that the sample contains carbon.[22,51] For the films with incorporated carbon, the 2100 cm$^{-1}$ peak is more dominant than the 2000 cm$^{-1}$ peak. This could either be caused by a material that is very rich in voids or, more likely, by a higher amount of

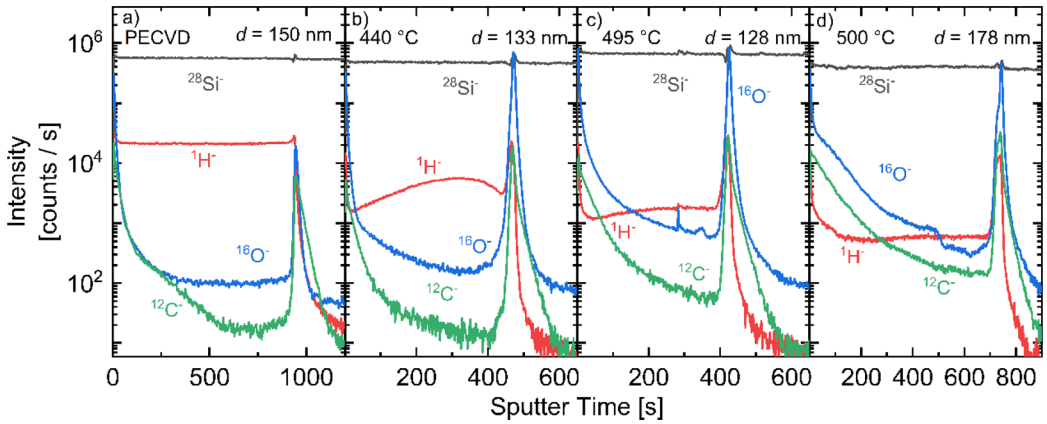


Fig. 6 Silicon, hydrogen, carbon, and oxygen SIMS profiles of (a) an intrinsic PECVD film and APCVD films deposited at (b) 440 °C, (c) 495 °C and (d) 555 °C.

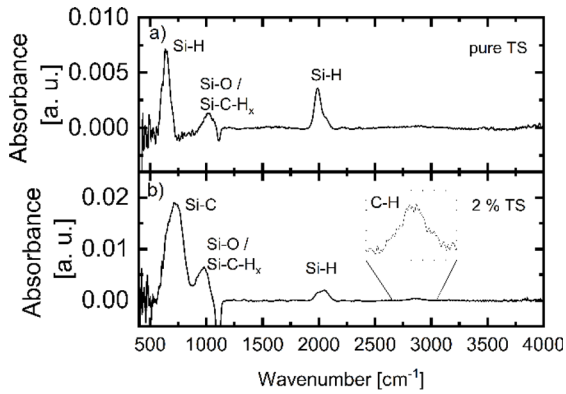


Fig. 7 FTIR spectra of (a) an a-Si:H film deposited at 440 °C with 20 µl trisilane for 10 minutes and (b) an a-Si:H film deposited at 555 °C with 440 µl of 2% trisilane diluted in cyclooctane for 10 minutes. The peaks are labeled with the corresponding bonds. In (b) the Si–H bending vibration peak at 640 $cm^{-1}$ is overlaid by the strong Si–C peak at around 720–780 $cm^{-1}$.

hydrogen bonded to silicon with a carbon back bond.[16,19,22,51] In addition, the peak at 900–1100 $cm^{-1}$ shifts slightly to a lower wavelength. The shift is likely due to a higher concentration of Si–C–$H_2$ modes compared to Si–O, which are probably dominant within the spectra of the purely deposited a-Si shown in Fig. 7a. In the following, we use the Si–C peak at 720–780 $cm^{-1}$ to quantify the carbon content within our a-Si:H films.

Fig. 8a shows conductivity, thickness, hydrogen content, microstructure parameter $R$ and density of Si–C bonds as a function of trisilane concentration in dilution samples deposited at 440 °C. Both $\sigma_d$ and $\sigma_{ph}$ as well as $c_H$ are mostly unaffected by cyclooctane dilution. In contrast, the microstructure parameter $R$ increases with a decreasing trisilane concentration for trisilane concentrations below 10%. In this series, the effect on the carbon content was not detectable with FTIR. However, SIMS measurements, shown in Fig. S2,† revealed a 3–4 orders of magnitude increase in carbon content compared to films made with pure silane. The H concentration varies only slightly between 6 and 8%. The scatter of the film thickness within the Dilution series is probably due to the manual precursor injection (*cf.* Experimental section).

Fig. 8b shows the material properties *vs.* the dilution ratio for films deposited at 495 °C. The figure shows that $c_H$ and $R$ increase with an increasing cyclooctane concentration for films made with less than 10% trisilane content. This trend might be due to the incorporated carbon, which is supported by the increasing Si–C vibrational peak located at 720–780 $cm^{-1}$. The increase in $c_H$, up to 6%, might be one reason for the increased photosensitivity observed in samples with trisilane concentrations below 10%. The difference in photosensitivity between 10% and 100% trisilane content is likely due to fluctuations in deposition conditions. A deposition temperature of 495 °C is close to the critical point where the photo-/dark conductivity splitting vanishes (as shown in Fig. 2a). Therefore, small differences in temperature or precursor amounts can have a significant impact on photosensitivity.

Fig. 8c shows the material properties *vs.* the dilution ratio for films deposited at 555 °C. For trisilane concentrations above 10%, no hydrogen is detected. However, at concentrations below 10%, a significant amount of hydrogen is present in the film, likely bonded to silicon with carbon back-bonds ($R = 1$). Despite this, the hydrogen does not seem to passivate defects, as the conductivities ($\sigma_{ph}$ and $\sigma_d$) remain similar across all films, regardless of hydrogen content.

A Si–C peak was observed for all dilution ratios. Even in pure trisilane deposition, enough carbon—likely from impurities in the glove box—was incorporated into the film, resulting in a noticeable peak in the FTIR spectrum. Reducing the trisilane concentration leads to increased carbon incorporation, reaching levels comparable to the silicon content ($10^{22}$ atoms per $cm^3$).

### Material deposited using highly diluted trisilane

We used a trisilane concentration of 2% in cyclooctane to investigate the influence of a high cyclooctane dilution on the a-Si:H film properties in more detail. As for the deposition using pure silane we made a temperature, deposition time and

 

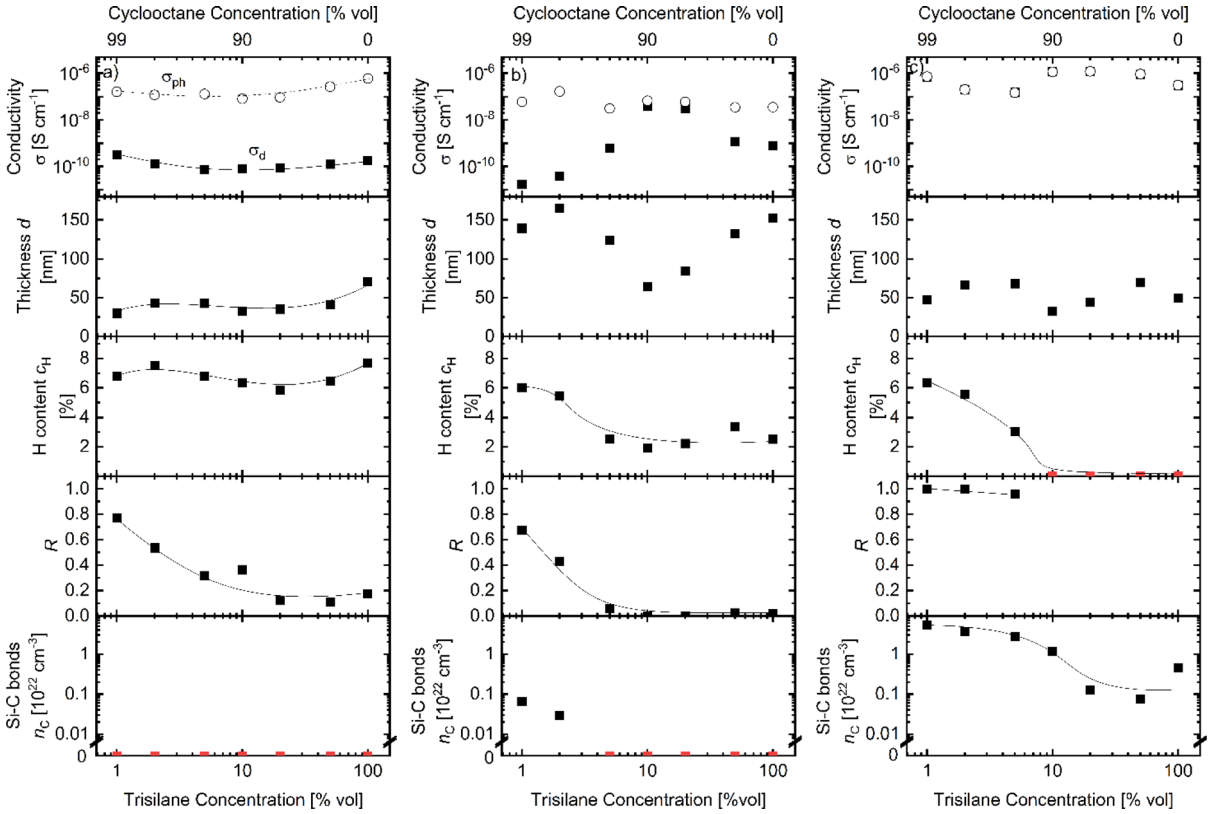


Fig. 8 Dark and photoconductivity $\sigma_d$ and $\sigma_{ph}$, thickness $d$, hydrogen content $c_H$, microstructure parameter $R$ and the amount of Si–C bonds $n_C$ of a-Si:H films as a function of the trisilane concentration within the precursor deposited at a deposition temperature $T$ of (a) 440 °C, (b) 495 °C and (c) 555 °C. The red marked points were set to 0, since the signal-to-noise ratio was too small to determine a peak within the FTIR spectrum. The lines are guides to the eye.

a precursor volume (Temp2, Time2, Amount2) series using the 2% trisilane solution. The deposition parameters of all three series are given in Table 1. The Time2 and Amount2 series were made at 470 °C since, at this temperature, the films have an appropriate balance between the high growth rate and high film quality (high $c_H$ and photosensitivity). The measurement results for the series are shown in Fig. 9.

Fig. 9a shows the results of the Temp2 series. The thickness of the films increases with increasing deposition temperature for $T < 525$ °C and remains almost constant for $T > 525$ °C. For all films, $R$ is higher than 0.4. The microstructure parameter $R$ decreases with increasing temperature for $T < 495$ °C, probably due to a lower proportion of H at the interface (which vibrates at a wavenumber of 2100 $cm^{-1}$) relative to the overall Si–H spectrum. In contrast, for $T > 495$ °C, $R$ increases, tentatively due to a carbon content increase leading to more Si–H bonds with C back-bonds. This more stable bonded H might also lead to a $c_H$ of 2% for layers deposited at $T > 495$ °C, instead of full H effusion. Beside the film deposited at $T =$ 580 °C, all films show a photoresponse with a maximum at 470 °C, probably because of the higher $c_H$ ($\sigma_d$ at 440 °C probably an outlier).

In Fig. 9b the results of sample series Time2 are shown. The photosensitivity varies with the deposition time with a maximum for the 10 min deposition. Accordingly, $c_H$ strongly increases from 2% to 6% and $R$ strongly decreases from 1 to 0.4 within the first 5 min. The film thickness data indicate that the growth rate first is approximately constant and then, for deposition times longer than 5 min, the growth rate decreases, due to depletion of the precursor. In addition, a longer deposition time leads to a higher incorporation of carbon and less inserted H into the film.

Fig. 9c shows the results of the sample series Amount2. An increased amount of precursor seems to increase the a-Si:H growth rate. This leads to a (linear) increase in the film thickness. The higher film growth is linked to an increase in photosensitivity and $c_H$. The higher growth rate is also accompanied by a lower carbon incorporation and lower $R$, probably because of fewer carbon back-bonds of Si–H vibrations.

For one film deposited at $T = 580$ °C using the solution with 2% trisilane, an ESR measurement was made, to analyze the $g$-factor, which is influenced by the SiC stoichiometry.[52] As shown in Fig. S1b,† the film with a thickness of 430 nm showed a $g$-factor of 2.004 which is closer to that of amorphous silicon carbide (a-SiC) (2.003) rather than a-Si (2.0055), in agreement with the high carbon content in the films.[52] The spin density of this sample was $1.35 \times 10^{19}$ $cm^{-3}$, which is slightly lower than that of the sample deposited with pure trisilane at $T = 555$ °C, possibly because of the increased $c_H$ and related passivation of

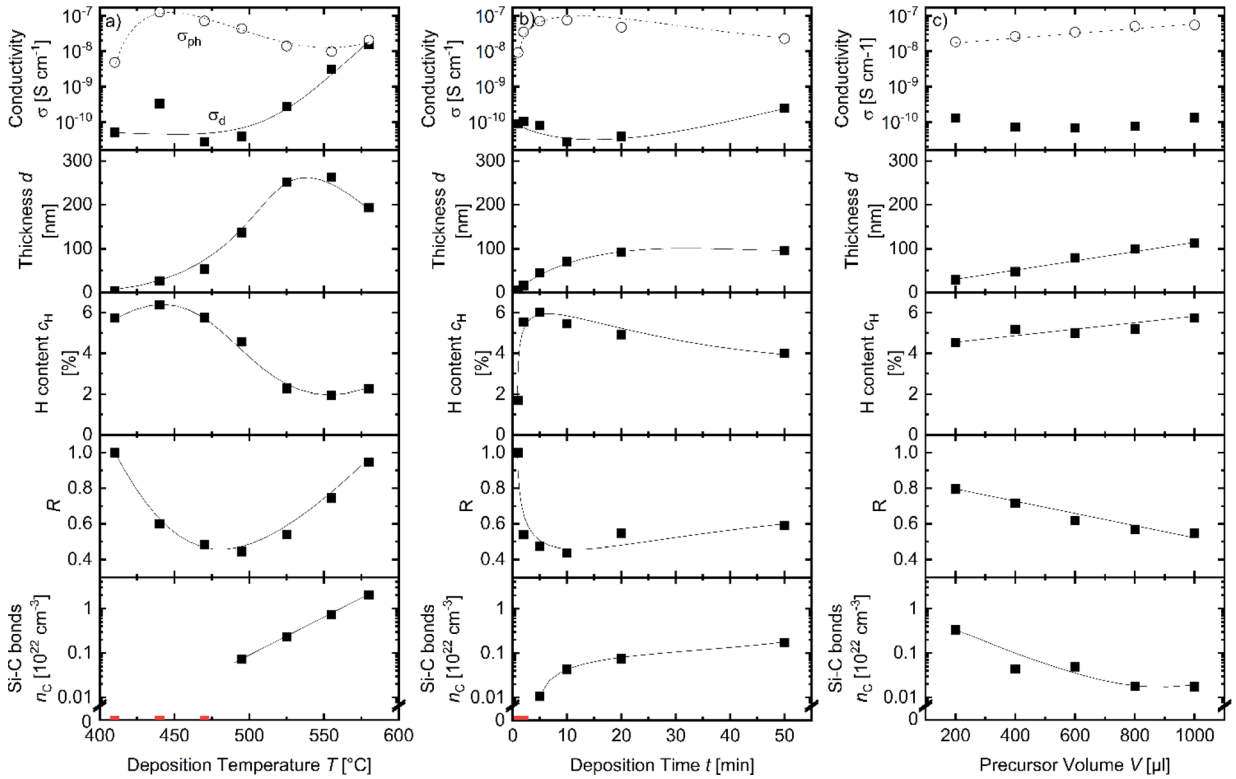


Fig. 9 Dark and photoconductivity $\sigma_d$ and $\sigma_{ph}$, thickness $d$, hydrogen content $c_H$, microstructure parameter $R$ and amount of Si–C bonds $n_c$ of a-Si:H films deposited with 2% trisilane diluted in cyclooctane as a function of (a) deposition temperature $T$, (b) deposition time $t$, and (c) precursor volume $V$. Deposition time and precursor amount were varied at a deposition temperature of $T = 470$ °C. The red-marked points were set to 0, since the signal-to-noise ratio was too small to determine a peak within the FTIR spectrum. The lines are guides to the eye.

defects for films deposited using high cyclooctane concentrations.

## Discussion

The films deposited with pure trisilane have properties and quality on par with a-Si:H films deposited with similar methods found in the literature. The best photosensitivity of $10^4$ found for films deposited at 440 or 470 °C is similar to or higher than the values of other films without H treatment investigated by Bedini *et al.*[11] and Masuda *et al.*[53] The purity of the low temperature a-Si:H films regarding oxygen and carbon incorporation is comparable with the purity of PECVD films, as shown in Fig. 6. Nevertheless, the lowest defect density measured by ESR was $3 \times 10^{18}$ cm$^{-3}$ which is rather high compared to standard PECVD films.[35] Masuda *et al.*[53] found spin-densities between $10^{17}$ and $10^{18}$ cm$^{-3}$ for films deposited with cyclopentasilane at a temperature between 360 and 420 °C.

We found a $c_H$ of less than 10% and a low $R$ in all films, which aligns with the fact that even the lowest deposition temperature used in this work is above the H effusion temperature.[34] The elevated temperatures result in a high hydrogen effusion rate during the growth process, particularly for hydrogen located in voids leading to a low $R$.[28] This suggests that the high defect density measured by ESR may stem from insufficient passivation and structural imperfections.[36]

In agreement with this, a clear correlation between the hydrogen concentration and the conductivity of the films was observed, consistent with the findings of Beyer and Wagner[36] and Fritzsche.[44] They suggested that a decrease in $c_H$ can cause an increase in defect densities, leading to a decrease in $\sigma_{ph}$.[35]

The a-Si:H films produced by our process are characterized by high purity, particularly in terms of low oxygen and carbon incorporation. However, the relatively low hydrogen content ($c_H$) in the films presents a challenge for some specific applications. For example, passivating layers of a-Si:H in silicon heterojunction (SHJ) solar cells are required to have higher hydrogen content for effective passivation. To address this issue, one potential solution is post-deposition hydrogenation.

For films deposited at high temperatures $T \geq 555$ °C, a small amount of H found in the a-Si:H films renders them highly suitable for various high-temperature processes, including recrystallization, as it significantly diminishes the risk of blistering. Therefore, this material shows strong potential for use as a precursor for polycrystalline silicon in TopCon solar cells.

A low $c_H$ (<2%) indicates that the deposition time of 10 min is long enough to remove not only all H at internal surfaces (2100 cm$^{-1}$ peak) but also almost all H atoms within the silicon-network.

In addition, the low $c_H$ and therefore high defect density seem to create a conductive defect band, which increases the $\sigma_d$

 

while also speeding up the recombination of photogenerated carriers, resulting in a photosensitivity of around 1.

The defect density increases one order of magnitude for a deposition temperature increase from $T = 440$ °C to 555 °C, probably as a result of less H incorporation into the film.[36]

With increasing deposition temperature, the O and C content increase as well, with an especially sharp increase near the surface, as shown in Fig. 6. This can tentatively be attributed to slower a-Si:H film deposition at the end of the deposition process, due to the depletion of the trisilane concentration during the growth process. This combined with the high temperature leads to a higher ratio of impurity radicals to silane radicals and therefore to a higher impurity incorporation. Therefore, for films deposited at high temperatures, in addition to a lack of H, oxygen impurities can lead to a higher amount of defects within the material as well.[47,54] Kinoshita *et al.*[54] showed a decrease in the conductivity with increasing oxygen content. However, they only found a minor reduction in the photosensitivity for very high oxygen contents up to $10^{21}$ atoms per $cm^3$, indicating that the reduction of the photosensitivity for high temperatures as shown in Fig. 2a is mainly a result of the low H content available for passivation within the film.

The origin of the C and O atoms can be the rest of organic solvents used for other film depositions within the chamber or impurity gases within the glove box such as $CO_2$, which is not monitored. The very steep increase in C and O counts at the surface of all samples, observed for sputter times >100 s in Fig. 6, can be attributed to impurities on the sample surfaces originating from the transportation of the samples in the ambient atmosphere.

By varying the deposition time and precursor volume, the film properties can be varied as well. A higher amount of precursor leads to a higher number of radicals that can interact with the substrate surface. The increased growth rate due to more radicals can lead to a higher incorporation of H and to a more porous or void-rich film, resulting in a higher $R$.[43] Increasing the deposition time in fact decreases the average growth rate and can lead to annealing effects. Both, a decreased growth rate and thermal annealing, reduce $c_H$ and $R$ for films deposited with pure trisilane.

The introduction of cyclooctane as a solvent for trisilane leads to significant carbon incorporation in the films, enhancing reproducibility by increasing the available precursor. Films grown with the 2% trisilane solution exhibit greater thickness, particularly at higher temperatures, due to more efficient precursor utilization. Specifically, 400 µl of the 2% trisilane solution (equivalent to 8 µl of trisilane) yields a thicker film compared to the 10 µl of pure trisilane.

At lower temperatures and cyclooctane concentrations, moderate carbon contamination has minimal impact on conductivity and $c_H$ but increases $R$ due to additional Si–H bonds with carbon back-bonds. At deposition temperatures above 495 °C and cyclooctane concentrations above 95%, key differences in film properties emerge. A higher carbon incorporation is accompanied by increased hydrogen incorporation and higher $R$, reflecting the bonding of H primarily to silicon atoms with carbon back-bonds.[17,22] Because of the effect of the added carbon on $R$, the $R$ values of films with higher carbon content cannot be directly compared to those of films made with pure trisilane.

Effusion experiments of a-SiC:H show a higher temperature stability of H in a-SiC:H than in a-Si:H,[28,55] in agreement with the fact that a higher carbon content of the films also leads to a higher H incorporation at high deposition temperatures.

Because of the higher H content, the carbon incorporation can improve the photosensitivity of the films deposited at temperatures between 495 °C and 555 °C. For films made of pure silane, almost no $\sigma_{ph}/\sigma_d$ splitting can be observed for this temperature regime.

The high Si–C peak in FTIR spectra and a $g$-value of 2.004 observed for a sample deposited at $T = 580$ °C and with 2% trisilane solved in cyclooctane as the precursor demonstrate that for films deposited at high temperature and with high cyclooctane concentrations the material configuration shifts from carbon-polluted a-Si:H to an a-Si:H/a-SiC:H mixture. The silicon-rich a-SiC:H matrix is a promising candidate as a precursor for nano-crystalline silicon embedded in an a-SiC matrix, which can be achieved through the process of annealing. This material has a wide applicability in optoelectronic applications.[56–60]

These results show that the use of cyclooctane as a solvent for silicon precursors can significantly influence the film properties. Nevertheless, we also showed that deposition temperatures and cyclooctane concentrations below 495 °C and 90%, as used for most liquid silane processes, are uncritical regarding C incorporation.[5,6,11]

## Conclusions

To progress in deposition of a-Si:H thin films using the liquid precursor trisilane, we build up a new APCVD system to pave the way for the industrial application of this process and to demonstrate the potential for using the layers in solar cells and other semiconductor components. The system is capable of controllable and reproducible deposition of a-Si:H films with a high quality compared to films made using similar systems. ESR and FTIR spectroscopy confirm that the material is amorphous silicon.

The microstructure, defect density and conductivity of a-Si:H change with the process parameters of the deposition system such as deposition temperature, deposition time, and precursor amount. Using pure trisilane, the hydrogen content and microstructure parameter can be varied in the range of 0–10% and 0–0.6, respectively. We found the lowest defect density of $3 \times 10^{18}$ $cm^{-3}$ and a photosensitivity in the order of $10^4$ for films deposited at $T = 440$ °C. It is therefore necessary to further improve the film quality with regard to hydrogen content and defect density in order to make it suitable for use in SHJ solar cells. However, for high temperatures such as $T = 555$ °C, the low H-content of the films presented here makes them a suitable candidate for high-temperature processes such as recrystallization, as the risk of blistering due to H accumulation is significantly reduced.

We investigated the influence of cyclooctane as solvent on the film properties and found a critical trisilane concentration of 10% diluted in cyclooctane and a critical deposition temperature of 495 °C. For lower trisilane concentrations and higher temperatures, we found a significant incorporation of carbon, leading to changes in the film properties such as an increased H content and a microstructure parameter increase up to 1. This also results in macroscopic changes such as an increase in the photoconductivity of the film, maybe allowing the fabrication of a-Si:H films with a higher heat stability. From FTIR spectra and ESR measurements, it can be concluded that for the highest dilutions and temperatures, the material can be regarded as a mixture of a-Si:H and a-SiC:H. SIMS measurements have shown that when deposition temperatures are below 495 °C and the trisilane content is 10% or higher, the carbon content in the films slightly increases. However, this carbon increase is not significant enough to affect the hydrogen content or the conductivity of the films.

## Data availability

The data supporting this article have been included as part of the ESI.†

## Author contributions

The research project was a collaborative effort, with each author contributing to specific roles. B. F. and M. N. jointly conceptualized the study design and defined the research objectives. Data curation was conducted by B. F. and O. A., who collected, organized, and curated the data for subsequent analysis. B. F. took charge of the formal analysis interpreting the results alongside M. N. and O. A. Securing the funding necessary to execute the research was the responsibility of U. R., R. A. E., S. H. and M. S. who successfully acquired the financial resources. The investigation phase was led by B. F., O. A., A. B. and P. J., who oversaw the experiments and investigations outlined in the study. Methodological frameworks and experimental protocols were developed by B. F. in collaboration with M. N. Project administration duties were shared among all authors, with B. F. coordinating and managing the overall project workflow. The provision of essential resources for the research was ensured by U. R., R. A. E. and M. S. M. N., S. H. and U. R. provided supervision, offering guidance throughout the project lifecycle. Visual representations of the data and results were created by B. F. and M. S. The initial version of the manuscript was drafted by B. F., with subsequent critical reviews and editing conducted by all authors to refine the intellectual content and enhance clarity.

## Conflicts of interest

There are no conflicts to declare.

## Acknowledgements

We sincerely thank Pascal Foucart and Udo Schürmann for their help in preparing the ToC-figure and the technical drawing of the setup for this paper. Their dedication and expertise have significantly enriched the visual presentation of our research findings.

## References

1 H. Sai, P. W. Chen, H. J. Hsu, T. Matsui, S. Nunomura and K. Matsubara, Impact of intrinsic amorphous silicon bilayers in silicon heterojunction solar cells, *J. Appl. Phys.*, 2018, **124**(10), 103102.
2 R. Ishihara, J. Zhang, M. Trifunovic, M. van der Zwan, H. Takagishi, R. Kawajiri, *et al.*, Single-Grain Si TFTs Fabricated by Liquid-Si and Long-Pulse Excimer-Laser, *ECS Trans.*, 2013, **50**(8), 49–53.
3 S. Han, X. Dai, P. Loy, J. Lovaasen, J. Huether, J. M. Hoey, *et al.*, Printed silicon as diode and FET materials – Preliminary results, *J. Non-Cryst. Solids*, 2008, **354**(19–25), 2623–2626.
4 B. Wu, C. Chen, D. L. Danilov, R. A. Eichel and P. H. L. Notten, All-Solid-State Thin Film Li-Ion Batteries: New Challenges, New Materials, and New Designs, *Batteries*, 2023, **9**(3), 186.
5 T. Bronger, P. H. Wöbkenberg, J. Wördenweber, S. Muthmann, U. W. Paetzold, V. Smirnov, *et al.*, Solution-Based Silicon in Thin-Film Solar Cells, *Adv. Energy Mater.*, 2014, **4**(11), 1301871.
6 T. Sontheimer, D. Amkreutz, K. Schulz, P. H. Wöbkenberg, C. Guenther, V. Bakumov, *et al.*, Solution-Processed Crystalline Silicon Thin-Film Solar Cells, *Adv. Mater. Interfaces*, 2014, **1**(3), 1300046.
7 Z. Shen, T. Masuda, H. Takagishi, K. Ohdaira and T. Shimoda, Fabrication of high-quality amorphous silicon film from cyclopentasilane by vapor deposition between two parallel substrates, *Chem. Commun.*, 2015, **51**(21), 4417–4420.
8 T. Masuda, H. Takagishi, Z. Shen, K. Ohdaira and T. Shimoda, Phosphorus- and boron-doped hydrogenated amorphous silicon films prepared using vaporized liquid cyclopentasilane, *Thin Solid Films*, 2015, **589**, 221–226.
9 P. V. Dung, P. T. Lam, N. D. Duc, A. Sugiyama, T. Shimoda and D. H. Chi, First-principles study of the thermally induced polymerization of cyclopentasilane, *Comput. Mater. Sci.*, 2010, **49**(1), S21.
10 A. P. Cádiz Bedini, L. D. Trieu, S. Muthmann, U. Rau and R. Carius, Approaching Solar-Grade a-Si:H for Photovoltaic Applications *via* Atmospheric Pressure CVD Using a Trisilane-Derived Liquid Precursor, *Sol. RRL*, 2017, **1**(7), 1700030.
11 A. P. Cádiz Bedini, S. Muthmann, J. Flohre, B. Thiele, S. Willbold and R. Carius, Sonophotolytically Synthesized Silicon Nanoparticle-Polymer Composite Ink from a Commercially Available Lower Silane, *Macromol. Chem. Phys.*, 2016, **217**(15), 1655–1660.
12 T. Shimoda, Y. Matsuki, M. Furusawa, T. Aoki, I. Yudasaka, H. Tanaka, *et al.*, Solution-processed silicon films and transistors, *Nature*, 2006, **440**(7085), 783–786.

 

13 H. Tanaka, H. Iwasawa, D. Wang, N. Toyoda, T. Aoki, I. Yudasaka, *et al.*, Spin-on n-Type Silicon Films Using Phosphorous-doped Polysilanes, *Jpn. J. Appl. Phys.*, 2007, **46**(10L), L886.
14 T. Masuda, N. Tatsuda, K. Yano and T. Shimoda, Silicon deposition in nanopores using a liquid precursor, *Sci. Rep.*, 2016, **6**(1), 37689.
15 B. Arkles, Y. Pan, F. Jove, J. Goff and A. Kaloyeros, Synthesis and Exploratory Deposition Studies of Isotetrasilane and Reactive Intermediates for Epitaxial Silicon, *Inorg. Chem.*, 2019, **58**(5), 3050–3057.
16 W. Beyer and M. S. A. Ghazala, Absorption Strengths of Si-H Vibrational Modes in Hydrogenated Silicon, *MRS Online Proc. Libr.*, 1998, **507**, 601.
17 T. Kaneko, D. Nemoto, A. Horiguchi and N. Miyakawa, FTIR analysis of a-SiC:H films grown by plasma enhanced CVD, *J. Cryst. Growth*, 2005, **275**(1–2), e1097–e1101.
18 B. Fischer, A. Lambertz, M. Nuys, W. Beyer, W. Duan, K. Bittkau, *et al.*, Insights into the Si–H Bonding Configuration at the Amorphous/Crystalline Silicon Interface of Silicon Heterojunction Solar Cells by Raman and FTIR Spectroscopy, *Adv. Mater.*, 2023, **35**(47), 2306351.
19 A. H. M. Smets, W. M. M. Kessels and M. C. M. van de Sanden, Vacancies and voids in hydrogenated amorphous silicon, *Appl. Phys. Lett.*, 2003, **82**(10), 1547–1549.
20 D. Jousse, E. Bustarret and F. Boulitrop, Disorder and defects in sputtered a-SiH from subgap absorption measurements, *Solid State Commun.*, 1985, **55**(5), 435–438.
21 A. H. Mahan, P. Raboisson and R. Tsu, Influence of microstructure on the photoconductivity of glow discharge deposited amorphous SiC:H and amorphous SiGe:H alloys, *Appl. Phys. Lett.*, 1987, **50**(6), 335–337.
22 D. S. Kim and Y. H. Lee, Room-temperature deposition of a-SiC:H thin films by ion-assisted plasma-enhanced CVD, *Thin Solid Films*, 1996, **283**(1), 109–118.
23 W. Duan, A. Lambertz, K. Bittkau, D. Qiu, K. Qiu, U. Rau, *et al.*, A route towards high-efficiency silicon heterojunction solar cells, *Prog. Photovoltaics*, 2022, **30**(4), 384–392.
24 C. Malten, *Pulsed Electron Spin Resonance of Amorphous and Microcrystalline Semiconductors*, Jülich: Forschungszentrum Jülich GmbH, 1996, p. 94.
25 M. Cardona, Vibrational Spectra of Hydrogen in Silicon and Germanium, *Phys. Status Solidi B*, 1983, **118**(2), 463–481.
26 M. H. Brodsky, M. Cardona and J. J. Cuomo, Infrared and Raman spectra of the silicon-hydrogen bonds in amorphous silicon prepared by glow discharge and sputtering, *Phys. Rev. B: Solid State*, 1977, **16**(8), 3556–3571.
27 Y. Ashida, Y. Mishima, M. Hirose, Y. Osaka and K. Kojima, Hydrogenated Amorphous Silicon Produced by Pyrolysis of Disilane in a Hot Wall Reactor, *Jpn. J. Appl. Phys.*, 1984, **23**(3), L129–L131.
28 W. Beyer and F. Einsele, Hydrogen Effusion Experiments, in *Advanced Characterization Techniques for Thin Film Solar Cells*, John Wiley & Sons, Ltd, 2016, pp. 569–95, available from DOI: **10.1002/9783527699025.ch20**.
29 W. Beyer, Infrared absorption and hydrogen effusion of hydrogenated amorphous silicon-oxide films, *J. Non-Cryst. Solids*, 2000, **266–269**, 845–849.
30 S. Yasuda, T. Chikyow, S. Inoue, N. Matsuki, K. Miyazaki, S. Nishio, *et al.*, Pulsed laser deposition of photosensitive a-Si thin films, *Appl. Phys. A*, 1999, **69**(1), S925–S927.
31 K. H. Lee, J. H. Yoo, B. Y. Moon, J. H. Jung, J. Jang, S. M. Pietruszko, *et al.*, Low temperature fabrication of APCVD a-Si thin film transistors with ion doped layer, *J. Non-Cryst. Solids*, 1996, **198–200**, 1141–1145.
32 S. Guruvenket, J. M. Hoey, K. J. Anderson, M. T. Frohlich, R. A. Sailer and P. Boudjouk, Aerosol assisted atmospheric pressure chemical vapor deposition of silicon thin films using liquid cyclic hydrosilanes, *Thin Solid Films*, 2015, **589**, 465–471.
33 H. Wagner and W. Beyer, Reinterpretation of the silicon-hydrogen stretch frequencies in amorphous silicon, *Solid State Commun.*, 1983, **48**(7), 585–587.
34 W. Beyer and H. Wagner, Hydrogen evolution from plasma-deposited amorphous silicon films, *J. Phys. Colloq.*, 1981, **42**(C4), C4.
35 O. Astakhov, R. Carius, F. Finger, Y. Petrusenko, V. Borysenko and D. Barankov, Relationship between defect density and charge carrier transport in amorphous and microcrystalline silicon, *Phys. Rev. B: Condens. Matter Mater. Phys.*, 2009, **79**(10), 104205.
36 W. Beyer and H. Wagner, The role of hydrogen in a-Si:H — results of evolution and annealing studies, *J. Non-Cryst. Solids*, 1983, **59–60**, 161–168.
37 H. A. Bosan, W. Beyer, U. Breuer, F. Finger, N. Hambach, M. Nuys, *et al.*, Investigation of Thermal Stability Effects of Thick Hydrogenated Amorphous Silicon Precursor Layers for Liquid-Phase Crystallized Silicon, *Phys. Status Solidi A*, 2021, **218**(9), 2000435.
38 K. Belrhiti Alaoui, S. Laalioui, Z. Naimi, B. Ikken and A. Outzourhit, Photovoltaic and impedance spectroscopy characterization of single-junction a-Si:H p–i–n solar cells deposited by simple shadow masking techniques using PECVD, *AIP Adv.*, 2020, **10**(9), 095315.
39 G. Lucovsky, R. J. Nemanich and J. C. Knights, Structural interpretation of the vibrational spectra of a-Si: H alloys, *Phys. Rev. B: Condens. Matter Mater. Phys.*, 1979, **19**(4), 2064–2073.
40 W. E. Hong and J. S. Ro, Kinetics of solid phase crystallization of amorphous silicon analyzed by Raman spectroscopy, *J. Appl. Phys.*, 2013, **114**(7), 073511.
41 M. Karaman, M. Aydın, S. H. Sedani, K. Ertürk and R. Turan, Low temperature crystallization of amorphous silicon by gold nanoparticle, *Microelectron. Eng.*, 2013, **108**, 112–115.
42 C. Smit, R. A. C. M. M. van Swaaij, H. Donker, A. M. H. N. Petit, W. M. M. Kessels and M. C. M. van de Sanden, Determining the material structure of microcrystalline silicon from Raman spectra, *J. Appl. Phys.*, 2003, **94**(5), 3582–3588.
43 R. A. Street, *Hydrogenated Amorphous Silicon*, Cambridge University Press, Cambridge, 1991.

44 H. Fritzsche, Characterized of glow-discharge deposited a-Si:H, *Sol. Energy Mater.*, 1980, **3**(4), 447–501.
45 J. M. Shannon and A. D. Annis, Current-induced defect conductivity in hydrogenated silicon-rich amorphous silicon nitride, *Philos. Mag. Lett.*, 1995, **72**(5), 323–329.
46 W. Beyer, Chapter 5 - Hydrogen Phenomena in Hydrogenated Amorphous Silicon, in *Semiconductors and Semimetals*, ed. Nickel N. H., Elsevier, 1999, vol. 61, pp. 165–239, available from: **https://www.sciencedirect.com/science/article/pii/S0080878408627076**.
47 J. Woerdenweber, T. Merdzhanova, R. Schmitz, A. Mück, U. Zastrow, L. Niessen, *et al.*, Influence of base pressure and atmospheric contaminants on a-Si:H solar cell properties, *J. Appl. Phys.*, 2008, **104**(9), 094507.
48 G. Lucovsky, A structural interpretation of the infrared absorption spectra of a-Si:H:O alloys, *Sol. Energy Mater.*, 1982, **8**(1–3), 165–175.
49 G. Lucovsky, J. Yang, S. S. Chao, J. E. Tyler and W. Czubatyj, Oxygen-bonding environments in glow-discharge-deposited amorphous silicon-hydrogen alloy films, *Phys. Rev. B: Condens. Matter Mater. Phys.*, 1983, **28**(6), 3225–3233.
50 A. O. Zamchiy, E. A. Baranov, I. E. Merkulova, S. Ya Khmel and E. A. Maximovskiy, Determination of the oxygen content in amorphous SiOx thin films, *J. Non-Cryst. Solids*, 2019, **518**, 43–50.
51 R. A. C. M. M. van Swaaij, A. J. M. Berntsen, W. G. J. H. M. van Sark, H. Herremans, J. Bezemer and W. F. van der Weg, Local structure and bonding states in a-Si1−xCx:H, *J. Appl. Phys.*, 1994, **76**(1), 251–256.
52 A. Morimoto, T. Miura, M. Kumeda and T. Shimizu, Defects in hydrogenated amorphous silicon-carbon alloy films prepared by glow discharge decomposition and sputtering, *J. Appl. Phys.*, 1982, **53**(11), 7299–7305.
53 T. Masuda, Y. Matsuki and T. Shimoda, Pyrolytic transformation from polydihydrosilane to hydrogenated amorphous silicon film, *Thin Solid Films*, 2012, **520**(21), 6603–6607.
54 T. Kinoshita, M. Isomura, Y. H. Y. Hishikawa and S. T. S. Tsuda, Influence of Oxygen and Nitrogen in the Intrinsic Layer of a-Si:H Solar Cells, *Jpn. J. Appl. Phys.*, 1996, **35**(7R), 3819.
55 S. S. Camargo, M. N. P. Carreño and I. Pereyra, Hydrogen effusion from highly-ordered near-stoichiometric a-SiC:H, *J. Non-Cryst. Solids*, 2004, **338–340**, 70–75.
56 U. Coscia, G. Ambrosone, S. Lettieri, P. Maddalena and S. Ferrero, Microcrystalline silicon–carbon films deposited by silane–methane mixture highly diluted in hydrogen, *Thin Solid Films*, 2006, **511–512**, 399–403.
57 D. Shan, D. Sun, M. Tang, R. Yang, G. Kang, T. Tao, *et al.*, Structures, Electronic Properties and Carrier Transport Mechanisms of Si Nano-Crystalline Embedded in the Amorphous SiC Films with Various Si/C Ratios, *Nanomaterials*, 2021, **11**(10), 2678.
58 Z. Wan, S. Huang, M. A. Green and G. Conibeer, Rapid thermal annealing and crystallization mechanisms study of silicon nanocrystal in silicon carbide matrix, *Nanoscale Res. Lett.*, 2011, **6**(1), 129.
59 D. Song, E. C. Cho, G. Conibeer, Y. Huang, C. Flynn and M. A. Green, Structural characterization of annealed Si1−xCx/SiC multilayers targeting formation of Si nanocrystals in a SiC matrix, *J. Appl. Phys.*, 2008, **103**(8), 083544.
60 D. Kar and D. Das, Conducting wide band gap nc-Si/a-SiC:H films for window layers in nc-Si solar cells, *J. Mater. Chem. A*, 2013, **1**(46), 14744–14753.

 